N 87-26023

COMPUTATIONAL CHEMISTRY

J. O. Arnold
NASA Ames Research Center
Moffett Field, CA 94035

ABSTRACT

With the advent of supercomputers, modern computational chemistry algorithms and codes, a powerful new tool has been created to help fill NASA's continuing need for information on the properties of matter in hostile or unusual environments. Computational resources provided under the NAS program have been a cornerstone for recent advancements in this field. Properties of gases, materials, and their interactions can be determined from solutions of the governing equations. In the case of gases, for example, radiative transition probabilities per particle, bond-dissociation energies, and rates of simple chemical reactions can be determined computationally as reliably as from experiment. The data are proving to be quite valuable in providing inputs to real-gas flow simulation codes used to compute aerothermodynamic loads on NASA's aeroassist orbital transfer vehicles and a host of problems related to the National Aerospace Plane Program. Although more approximate, similar solutions can be obtained for ensembles of atoms simulating small particles of materials with and without the presence of gases. Computational chemistry has applications in studying catalysis, properties of polymers, etc., all of interest to various NASA missions, including those previously mentioned. In addition to discussing these applications of computational chemistry within NASA, the governing equations and the need for supercomputers for their solution is outlined.

INTRODUCTION

The availability of large-scale computers at the NASA Ames Research Center during the past decade has been a key element in developing an aggressive effort by NASA to use a computational approach to provide reliable information on the properties of gases, materials and their interactions. The impact of this effort has been growing rapidly as a result of continuing advances in computational methods and, concurrently, with increases in computer speed and memory. Specifically, the advanced computational capabilities being provided for this endeavor through the Numerical Aerodynamic Simulation (NAS) program have markedly increased the utility of computational chemistry as practiced at NASA Ames. Further, this resource is also providing benefits to the international community by enabling advanced state-of-the-art benchmark calculations which assess the reliability of approximate approaches that require less computational power.

The objectives of Ames' computational chemistry activities are specified in figure 1. The gas phase studies provide computed properties of isolated atoms and molecules, and rates of chemical reactions which occur between them. Systems composed of one to eight atomic nuclei and up to 30 electrons are treated rigorously by solving the Schrodinger equation for the quantum mechanical interaction energy of the electron in the field of all atomic nuclei. Typical molecular properties computed are potential energy surfaces for ground and excited electronic states (i.e., the set of electronic energies for all atomic geometries), equilibrium geometries, probabilities for transitions between electronic states and molecular spectra. Rate constants for chemical reactions are computed by solving Hamilton's classical equations of motion for a potential energy surface obtained from the aforementioned solutions of Schrodinger's equation.

The gas/solid calculations begin with solutions of wavefunctions and total energies for "atomic clusters" such as those illustrated for a diatomic molecule interacting with an inverted pyramid of five metal atoms. In such calculations, the metal atoms are sometimes held fixed at spacings corresponding to the bulk surfaces to simulate gas-surface interactions at the atomic scale. The quantal calculations usually account only for the outer valence electrons since all-electron calculations are too large even for machines like the Cray 2. Such calculations have progressed to the point of considering its application to systems as large as $Ni_{25}O_5$ or $Fe_{64}H$. In addition to providing information on clusters of this size, interatomic forces deduced from these calculations are used as input to atomistic simulations of large ensembles of up to 10,000 atoms. These calculations provide better simulation of the interaction of gases and bulk surfaces, as shown on the far right of figure 1. Obviously, going from left to right (fig. 1), the systems grow enormously, and the reliability of the calculations range from being competitive with the best experiments available, to being helpful in interpreting experimental findings and suggesting solutions to materials problems of crucial National concern. This work constitutes the computation of properties of matter and the results are being used in a broad range of applications that are of current concern to NASA.

The gas phase work has great utility in providing inputs to chemically reacting, radiating, real-gas flow-field simulations like those which will occur about future space-based aerobraking orbital transfer vehicles (AOTVs). These vehicles will move men and materials between low and high Earth orbits and the Moon and Mars. These vehicles will fly very high (above 60-70 km) in the atmosphere during their aerobraking maneuver at speeds of approximately 9-13 km/sec. Under these conditions, as much as 10-15% of the gaseous species will be ionized.

Another program of National importance which requires the basic information on the properties of shock-heated air, as well as information on the hot air/hydrogen combustion process, is for the National Aerospace Plane (NASP). The NASP, in various implementations, will be capable of taking off from a conventional airport, cruising at Mach 5-12 (Los Angeles to Tokyo in 2 hr) or going into low Earth orbit, and returning to any other airport on Earth.

Discussions of the exciting missions of these vehicles and their future importance can be found in the report to the President by The National Commission on Space (1986).

Each of the missions discussed above, and others involving hypersonic flight require knowledge of the properties of materials and how they behave in the presence of hot gases or other hostile environments. For example, flight experiments on the Space Shuttle (Stewart et al., 1983) have shown that the thermal protection system (TPS) catalytic efficiency for recombination of boundary-layer atomic species effects the local heat transfer, i.e., a highly catalytic metal must absorb the diatomic heat of molecular recombination. On the other hand, a low-catalytic efficiency ceramic material such as the shuttle tile inhibits the recombination process, thereby preventing this heating and thus reducing the TPS weight requirement. Computational chemistry is helping us understand the differences in catalytic and noncatalytic materials. Such understanding clearly has the potential to aid in the development of new classes of advanced thermal protection materials for aerospace applications.

COMPUTATIONAL METHOD

Schrodinger's equation for gaseous molecules and atomic clusters is usually solved under the assumption that electronic motion is very fast compared with that of the constituent nuclei, allowing one to solve for the electronic degrees of freedom separately. Potential curves or surfaces are mapped out by obtaining several solutions corresponding to differing internuclear separations. (The time-independent form of the equation is studied for the determination of the properties previously mentioned.)

Figure 2 illustrates the approach (generally known as "ab-initio" in the field) for a diatomic molecule where the Hamiltonian contains a ∇_i^2 operator that corresponds to the electronic motion of the ith electron, the Z/r_{iA} terms account for electron-nuclear attraction and the $1/r_{ij}$ term accounts for electrons-electron repulsion, Ψ_e is the electronic wave function and E is the electronic energy, both being sought in the solution. The expansion approach assumes that the wave function can be expanded in terms of configuration state functions (CSFs) constructed from Slater determinates composed of unknown molecular orbitals, ϕ_i. The orbitals are taken to be linear combinations of either Gaussian (GTO)- or Slater (STO)-type atomic orbitals. The GTOs or STOs used in an n-particle molecular problem are often referred to as the one-particle basis set. The solution first involves selecting a STO- or GTO-basis set, and the quality of the solution depends critically upon this choice.

The next step involves evaluating spatial integrals for the one-particle basis set and sorting for the subsequent determination of the coefficients for the molecular orbitals, c_{ip}, and the expansion coefficient, a_K. The a_K coefficients weigh the importance of a CSF to the total wave function, Ψ_e. The number of CSFs used in a calculation can range from one (self-consistent field SCF) to more than 10 million (configuration interaction CI). The CI calculation, called electron correlation, accounts for the instantaneous repulsion each electron feels, and to all other electrons constituting the molecule. The CI calculation is an eigenvector-value problem in which one gets the lowest eigenvalue by an iterative numerical procedure.

For the purpose of discussion, assume that a quality calculation may involve a basic set of size M (generally $M = 50\text{-}100$). The order of the subsequent steps is specified in figure 2, and the corresponding times, in seconds, of a calculation for a single internuclear separation of a typical diatomic molecule are also shown on the figure. Note that the possible number of CSFs, each corresponding to a different occupation of electrons within the possible orbital space, grows as M^6. Clearly, these calculations use large amounts of computer resources. Reasonable progress with our computational chemistry program will continue to require sizable percentages of the Ames Central Computing Facility (CCF) and NAS resources. As the available computer power grows, the utility of computational chemistry will also grow, continuing to add insight into the nature of matter, and changing the way we conduct experiments.

BENCHMARK CALCULATIONS

In the past, expansions involving all possible CSFs (or full configuration interaction (FCI) calculations) were generally not possible except for two- or three-electron single-atoms and molecules. Work on larger systems with reasonably sized, atomic basis sets were truncated because of limitations in computer memory and speed. Bauschlicher, Langhoff, Taylor, and Partridge have recently been using the NAS Cray 2 to study the impact of truncating the number of CSFs for small molecular systems, and these are serving as benchmarks for the international computational chemistry community. In one of these studies, Bauschlicher and Langhoff (work submitted, Chemical Physics and Letters, 1986) first carried out full CI calculations on the molecular ground states of CH, NH, and OH, using a modest one-particle GTO basis for each molecule. The full CI calculations accounted for each and every possible occupation of the electrons within the n-particle basis.

For NH, the FCI calculations were conducted with a one-particle [5s4p2d/4s2p] GTO basis and involved 9,240,000 Slater determinants (37,110,150 CSFs) and required 8,000 sec of Cray 2 time/iteration to optimize the expansion coefficients. These FCI calculations and similar calculations for CH and OH were compared against the standard high-quality complete active space, self-consistent field/multiple reference singles and doubles configuration interaction CASSCF/MRSDCI. The CASSCF approach is one in which an active space is defined, and all configurations possible within this space are included in a calculation to determine the molecular orbital coefficients defined above. These molecular orbitals are then used in a CI calculations in which all configurations corresponding to single and double electronic excitations from any of the CASSCF configurations are included. Finally, a very small correction to account for the missing configurations corresponding to higher-order excitation is applied. For the modest-basis set calculations, only small differences (.015 eV max) in dissociation energies between the FCI and CASSCF/MRSDCI + Q computed results were noted, as can be seen from the tabulations in figure 3. These calculations clearly indicate that the standard truncated approach widely used and previously calibrated against experimental results (of which accurate ones are available) yield quality results.

In addition to these benchmark calculations, Bauschlicher and Langhoff also used a good quality basis set in conjunction with larger MRSDCI + Q calculations (Q = Quadruples) to predict values of the bond-dissociation energy for CH, NH and OH. As can be seen from the results shown in figure 3, Bauschlicher and Langhoff achieved chemical accuracy for CH and OH, for which accurate experimental data exist. On the basis of their calculations and estimates of the remaining error caused by basis set incompleteness, they recommend a dissociation energy of 3.37 ± .03 eV for NH and assign a 99% confidence limit to this value. This illustrates how computational chemistry is complementing the experimental approach in determining molecular properties, such as the bond-dissociation energy.

CALCULATION OF RADIATIVE PROPERTIES FROM FIRST PRINCIPLES: DIATOMIC MOLECULES

Figure 4 illustrates the computational procedure used to determine the radiative properties of molecules. The first step is to solve the Schrodinger equation for the electronic energy, E, and the wave function, Ψe, using the internuclear separation as a parameter as previously described. Potential-energy curves for the low-lying electronic states from a typical molecular calculation are shown on the left side of the chart. One can compute other electronic properties from the electronic wavefunction, such as the transition moments, which control the total strength of the transition between two electronic states, and the spin-orbit matrix elements, which control molecular and spectral fine structure. Once this is done, the next step is to solve the Schrodinger equation for the vibration-rotation motion. Then, by summing the product of the transition moments and the vibrational-rotational wavefunctions for all upper and lower states, one obtains the total cross section. The cross section shown on the right-hand side of figure 4 is for all the transitions between the potential-energy curves given on the left-hand side of the figure. The banded structure in the cross-section plot corresponds to bound-bound transitions and the underlying continuum corresponds primarily to transitions between bound and repulsive states (i.e., those with no minimum in the energy curve). The computated data for transition probabilities and spectral intensities are comparable to those from high quality experiments.

The cross sections yield the radiative intensity per molecule per excited state. Combining them with the appropriate distributions of species and excited states yields spectral and integrated intensity predictions in gases either in equilibrium or thermochemical nonequilibrium environments.

Thus, one can obtain a first principles absorption or emission spectrum of molecules which can be used as an input for the various flow-field codes which predict absorption, radiative heating, etc. These data are of key importance as inputs to fluid-flow simulations which predict radiative heating for the AOTV missions previously discussed. Radiative properties are also required for predictions of heat transfer in scramjet-combustor flows for the NASP and development of wind tunnel nonintrusive-flow diagnostics.

CALCULATION OF REACTION-RATE CONSTANTS

Rate constants for chemical reactions can be computed from first principles provided one is given the potential-energy surface resulting from the solution of Schrodinger's equation at all possible values of the interatomic coordinates.

A two-dimensional representation of such a potential surface for the reaction $N+O_2 \rightarrow NO+O$, recently computed by Walsh and Jaffe (1986), is shown on the left side of the figure (fig. 5). The surface corresponds to the N atom approaching the O_2 molecule at an angle of 110°. The diatomic potential curve for O_2 is recognizable at the left-hand side of the potential surface grid. Similarly, the potential curve for molecule NO can be seen on the lower-right-hand corner of figure 5 which corresponds to this diatomic leaving the O atom after the reaction occurs. The union of these limits with short bond distances between all three constituent atoms corresponds to the triatomic molecule NOO. The R_{NO} and R_{OO} coordinates correspond to bond distances between atoms while the electronic energy E increases in the vertical direction. Reactive trajectories on this surface are simulated by solving Hamilton's equations of motion written on figure 5 in which P_i are momenta and Q_i are the generalized coordinates, and $V(\tilde{Q})$ is a function representing the potential-energy surface. Many solutions corresponding to different initial vibrational states and approach conditions (orientation, impact parameter, etc.) are simulated giving rise to computed reaction cross section. By averaging these cross sections over the appropriate vibrational and rotational distribution (vibrational and rotational temperatures for the reactant O_2) and collision-energy distribution (translational temperature) one can determine rates of reactions as shown on the right-hand side of figure 5.

MOLECULAR-EXCITATION CROSS SECTIONS

Flow fields on AOTVs exhibit nonequilibrium, chemically reacting and radiative flows in which radiating heating is an important consideration in the design of the forebody heat shield. These flows are also weakly ionized. Preliminary analyses indicate that the collision of electrons with molecules is a very important mechanism for the production of the vibrationally and electronically excited molecules from whence flow-field radiation originates. Accurate flow simulations must account for the number density of excited-state molecular species, which depends upon the cross section for electron-molecule collisions. Computational chemists are using these techniques to provide this information, which has not been reliably provided by experimentation. Lima et al. (1986) have studied these cross sections using a Schwinger multichannel formulation, and validated against high quality experiments obtained on H_2. Figure 6 shows the comparison of the theoretical differential cross sections for the electron impact excitations of molecular Nitrogen, $e^- + N_2(X^1\Sigma_g^+) \rightarrow N_2(B^3\Pi_g) + e^-$, at an impact energy of 10 eV versus the scattering angle in degrees. Clearly there is a dramatic difference in the angular distribution resulting from the two available experimental studies (Mazeau et al., 1973 and Cartwright et al., 1977), although there is rough agreement in the magnitude of the cross sections between 60 and 120°. The first-principal quantal calculation is also shown. The cross section agrees with the magnitude in this region, and tends to support the experiments by Cartwright et al. (1977).

Results for the total cross section as a function of impact energy for this process are shown in figure 7. In this figure, four sets of experimental data are available (Cartwright et al., 1977, Borst and Chang, 1973, McConkey and Simpson, 1969, and Shemansky and Broadfoot, 1971) and shows that these data differ roughly by a factor of five, and which also exhibit different dependences on collision energy. The computational results again support Cartwright's data, and are consistent with the results for the differential cross sections discussed above.

These theoretical results (while using some approximations) clearly demonstrate the capability of ab-initio methods to predict collision cross-sections and illustrate their value in evaluating experimental data.

STUDIES OF ATOMIC CLUSTERS

As mentioned in the introduction, the quantum/classical approach, which works well for gases, is also being used in studies of the properties of materials and their interactions with gases. The favored geometrical orientation of an ensemble of metal atoms corresponds to that structure with the lowest total energy. For a small number of atoms (less than about 75), this property is amenable to the total energy calculations by quantal means as previously outlined, if one assumes that the inner electrons of each atom can have its presence accounted for by effective core potentials. These calculations are reliably determined in separate ab-initio calculations on isolated atoms. Alternatively, the classical approach (given interatomic forces as input) uses solutions of Hamilton's equations of motion to describe the behavior of the constituent atoms (up to 10,000 atoms can be included). The interatomic forces are assumed to be given as a summation of n-body interactions but of which only the two-body and three-body terms are retained. These forces have previously been determined from bulk or surface properties for pure metals, but in general have been difficult to obtain for mixtures of elements. Recently, Pettersson et al. (1986) have completed a dual study in which they compared predicted geometry for a series of aluminum-atom clusters using the results of both quantal and classical approaches on the same clusters of aluminum atoms.

The objective of the Pettersson et al. (1986) work was to find an alternative approach to the very large and computationally expensive ab-initio methods used to determine the properties of clusters and to extend the calculations to much larger clusters. In this study, the structure and stability of aluminum clusters containing from 2-6 and 13 atoms were calculated using both the ab-initio, quantum chemical approach and the classical atomistic simulations using a simplified parameterized interaction potential function. For each cluster, several different states and structures were considered. Two-dimensional structures were found by both methods to have the lowest energy up to Al_5. Figure 8 illustrates the different Al_6 structures considered. The two D_2h (D_2h hexagonal and D_2h triangular) and the C_2h structures are three-dimensional (3-D). The lowest energy structure according to the ab-initio calculations is the 3-D octahedron (O_h) while the parameterized modeling method predicts the planar C_{2h} to be the lowest-lying structure. However, the energy difference between the 3-D and planar structures is very small. Since the electron correlation energy is substantially larger for the 3-D O_h structure than for the planar one, the difference may be due to the method/level at which the correlation is treated and of which is currently under investigation.

For Al_{13}, only selected structures were calculated using the ab-initio methods. While the icoshedral structure had the lowest energy, the planar structure, D_{6h}, (predicted by the modeling method to be the lowest) was found to be low-lying and nearly equal in energy to the icoshedral structure. Otherwise, the calculated ordering of the structures was the same for both methods. Since there was only a small energy difference between the 3-D and planar Al_{13} structures, the three-body term in the modeling approach was systematically adjusted in an attempt to duplicate the ab-initio results (the value of the three-body term previously used was not necessarily the optimum value). This value was then used to predict the lowest-lying structure of Al clusters for up to 17 atoms. Figure 9 shows the results of these calculations for Al clusters containing from 7-15 atoms. Clusters with 7, 8, 10, and 12 atoms are planar. All clusters with 13 or more atoms are 3-D.

These calculations by Pettersson et al. (1986) show very promising results. First of all, they clearly demonstrate the need to account for three-body forces in the classical calculations. Secondly, with the three-body term included, the relative stabilities of all of the structures considered were correctly predicted with only two exceptions. Finally, the parameterized modeling approach should allow the study of substantially larger clusters (than can currently be treated by ab-initio methods) and enable predictions of the effects of temperature and characterization of vibrational frequencies. In addition, the computational cost of this method is significantly less than the previous approaches.

DISSOCIATION OF H_2 ON THE NI(100) SURFACE

Figure 10 displays an example of the ability and power of computational chemistry to study and predict gas-surface interactions. The figure shows the results of calculations (Bauschlicher et al., 1984) used to predict the dissociation of H_2 on a Ni(100) surface. Experimental studies have shown that certain molecules dissociate on some metallic surfaces but not on others. This calculation was performed to predict the activation energy for dissociation and to determine the role of metal d-electrons (electrons with multiple lobes and high angular momentum) in the dissociation process. The calculations used a Ni_{14} cluster, shown on the left side of the chart, to represent the metal surface. (The 14th Ni atom, not shown, lies below those shown in a third layer. Consequently, the Ni surface is represented by the base of an inverted equilateral pyramid.) The hydrogen-molecule (represented by the two small particles in the figure) was allowed to interact with each of the possible site locations on the surface. The hydrogen-molecule is shown in figure 10 in an "on-top" site since this location is the preferred site with the lowest barrier for dissociation. The figure on the right side of this chart is a potential contour of the hydrogen molecule in an "on-top" site. The top of the figure represents a diatomic-molecule approaching the Ni surface. As the molecule gets close to the Ni surface it interacts with the surface and dissociates as illustrated.

By turning the d-electrons "on" and "off", Bauschlicher et al. (1984) showed that the d-electrons play a significant role in the dissociation process and their presence reduces the computed dissociation barrier by 44 kcal/mole. The computed barrier for dissociation of 4kcal/mole ±3 is in good agreement with the experimental value of 0-1 kcal/mole. Further, the computed results show that once dissociated, the chemisorbed H atoms do not interact with the d-electrons, and these findings are also consistent with experiment. Finally, these calculations are capable of providing great insight into the catalytic nature of materials, and future studies will be directed toward developing a fundamental understanding of catalytic processes.

PROPERTIES OF POLYMERS

NASA is interested in advanced polymers for new aerospace applications. The Ames Computational

Chemistry group undertook studies several years ago to develop a program in which the computational approach could compliment NASA's ongoing experimental program for polymer development. Many macroscopic properties of polymers depend upon their molecular structure and upon the motions of their constituent subgroups. Calculations of polymers have been undertaken for model compounds which represent selected polymers in an attempt to relate their macroscopic- and molecular-level properties. These calculations use the single-configuration SCF method since it was previously demonstrated that this approach could give quantitative information on the torsional potentials corresponding to rotation of subgroups about chemical bonds. Several systems were studied, and it was concluded by Laskowki et al. (1986) that the energy differences between rotated groups can be generally determined to an accuracy of about 0.5 kcal/mol (150-200 cm^{-1}) and that torsional barriers can be determined to an accuracy o< 1.0 kcal/mole (300 cm^{-1}).

Figure 11 is an example of the calculations by Laskowski et al. (1986) compared with an experiment in which the geometries and energies of the methacryloyl fluoride were studied; specifically, rotations of the COF group about the C_2 - C_3 bond as shown on the figure.

As can be seen from the figure the energy differences at values of $\xi = 0°$ and 180° are in excellent agreement with the experimental data. The torsional potential for the COF group rotation about the C_2 - C_3 bond was determined by computing the energy defined by interpolating between the two geometries. Note that the computed torsional barrier is somewhat higher than the experimental results. However, it is believed that experimentally determined barrier heights are likely to be underestimated and that the theoretical values are likely to be more accurate.

In the same paper, Laskowski et al. (1986) also report studies of the 2-Methyl 2-carbonmethoxy butane molecule shown in figure 12, which is a monomer model of PMMA. Experimentalists originally believed that a high-energy transition in the molecule arose from the rotation of the ester side chain corresponding to the angle Ψ_2. However the calculations by Laskowski et al. showed that the observed peak is due to the rotation of the smaller methoxy group (Ψ_3) in figure 12. Subsequent to these calculations, new temperature-dependent nuclear magnetic resonance (NMR) measurements confirmed the computations, and it was established that the original experimental assignments were incorrect.

The initial study of quantum chemical calculations were on small-model compounds and macroscopic properties and measurements. For a system in which the molecular-level motions were localized (i.e., involved a single segment of the polymer). The current effort is being applied to another prototype system in which the motions are not localized -- the large amplitude motion of the relaxation process in polycarbonate. It is believed that the ability of this polymer to undergo large amplitude motions in the glassy state at very low temperatures (i.e., -100° C) is the origin of its high-impact strength (toughness).

Jaffe and Laskowski (work to be published) have undertaken SCF-level calculations of the geometries, energies and vibrational frequencies of various polycarbonate models to identify all possible stable conformers and the barriers for their interconversion. Most of these calculations used minimal basis sets (currently the use of larger basis sets is not feasible for such large compounds). However, they have found this approach to yield fairly good geometries (with known correction factors) and extremely good relative energies. The model compounds studied include diphenyl carbonate (DPC), and 2,2-diphenyl propane (DPP). The polycarbonate chain consists of alternating DPC and DPP components. This work to date has successfully predicted the most stable conformers, related the motion of the phenyl rings to coupling strength, and predicted both energy differences for selected geometries and torsional barriers.

A first step in modeling the macroscopic properties of polycarbonate has also been taken using a statistical model. The computed fragment geometries and conformer energies are used to construct the partition function for a model polymer chain of length 100,000 segments. From this model, the average chain extension can be determined and the bulk viscosity computed. The computed value of 1.18 at 25° C compares favorably with the experimentally determined value of 1.28 + 0.19. Previously Yoon and Flory (1981) had obtained values of 0.84 - 1.1 using a similar model that included adjustable parameters. They could adjust the model to "agree" with any experimental result (an older experimental study gave a value of 0.78), but they could not test the accuracy of the model nor could they use the model for predictive purposes. Here again, computational chemistry is complementing the experimental approach in developing a fundamental understanding of the properties of materials.

SUMMARY

The approach and illustrative example of work by the Ames Computational Chemistry Branch have been discussed. Currently, the results of this work is finding application in filling NASA's need for information on the properties of matter in hostile and unusual environments such as in the flow field about and on the surface of vehicles moving at hypervelocity speeds in the Earth's atmosphere.

Computational chemistry has changed the way NASA supplies its need for gas properties (much more reliance on results calculated with codes validated against experimental results) and has affected our level of understanding of materials properties.

The field of computational chemistry clearly has a great promise of expanding its importance and utility provided that computational speed and memory continue to increase as is being championed by the NAS program.

References

Bauschlicher, C. W., Jr.; Siegbahn, P. E. M.; and Blomberg, M. R. A.: The Dissociation of H_2 on the Ni(100) Surface. J. Chem. Phys., vol. 81, 1984, p. 2103.

Borst, W. L.; and Chang, S. L.: Excitation of Metastable $N_2(A^3\ \Sigma^+_\mu)$ Vibrational Levels by Electron Impact. J. Chem. Phys., vol. 59, 1973, p. 5830.

Cartwright, D. C.; Chutjian, A.; Trajmar, S.; and Williams, W.: Electron Impact Excitation of the Electron States of N_2 I. Differential Cross Section at Incident Energies from 10 to 50 eV. Phys. Rev. A., vol. 16, 1977, p. 1013.

Laskowski, B. C.; Jaffee, R. L.; and Komornicki, A.: Theoretical Study of the Conformational Properties and Torsional Potential Functions of Polyalkylmethacrylate Polymers. Applied Quantum Chemistry, Smith, V. H. et al. (eds.), D. Reidel Publishing Co., 1986.

Lima, M.; Luo, Z. P.; Hagano, S.; Pritchard, H.; McKoy, V.; and Huo, W. M.: Study of Electron-Molecule Collisions, Proceedings of the Indian Society of Atomic and Molecular Physics, 1986.

Mazeau, J.; Gresteau, F.; Hall, R. I.; Joyez, G.; and Reinhadt, J.: Electron Impact Excitation of N_2 I. Resonant Phenomena Associated with the $A^3\ \Sigma^+_u$ and $B^3\ T1_g$ Valence States, J. Phys. B., vol. 6, 1973, p. 867.

McConkey, J. W.; and Simpson, F. R.: Electron Impact Excitation of the $B^3\ Tl_g$ State of N_2, J. Phys. B., vol. 2, 1969, p. 923.

Pettersson, L. G. M.; Bauschlicher, C. W., Jr.; and Halicioglu, T.: Small Aluminum Cluster II Structure Binding in Al_n (n + 2-6, 13), J. Chem. Phys., 1986. (To be published).

Pioneering the Space Frontier, The Report of the National Commission on Space, Bantam Books, 1986.

Shemansky, D. E.; and Broadfoot, A. L.: Excitation of N_2 and N^2_+ Systems by Electrons-- II Excitation Cross Sections and $N_2$1PG Low-Pressure Afterglow, JQSRT, vol. 11, 1971, p. 1401.

Stewart, D. A.; Rakich, J. V.; and Lenfranco, M. J.: Catalytic Surface Effects on Space Shuttle Thermal Protection System During Earth Entry of Flights STS-2 through STS-5, AIAA Conference on Shuttle Performance, "Lesson Learned," Langley Research Center, Hampton, VA, Mar. 1983.

Walsh, S. P.; and Jaffee, R. J.: Calculated Potential Surfaces for the Reactions: O + N2 → NO + N and N + O2 → NO + O, J. Chem. Phys., 1986. (To be published).

Yoon, D. Y.; and Flory, P. J.: Intermediate Angle Scattering Functions and Local Chain Configurations of Semi-Crystalline and Amorphous Polymers, Polymer Bulletin, vol. 4, 1981, p. 693.

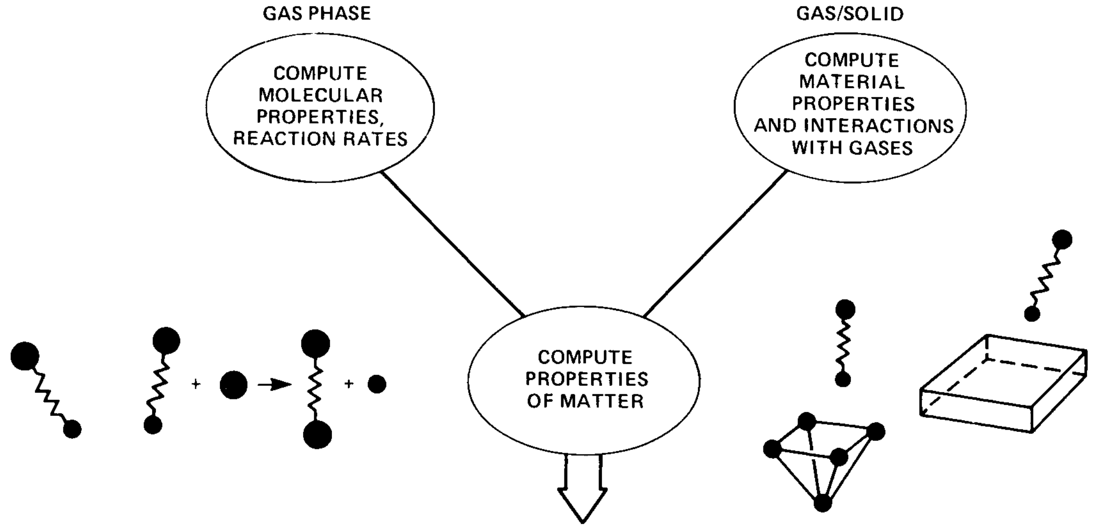
GAS PHASE
COMPUTE MOLECULAR PROPERTIES, REACTION RATES
GAS/SOLID
COMPUTE MATERIAL PROPERTIES AND INTERACTIONS WITH GASES
+
+
COMPUTE PROPERTIES OF MATTER

BASIC RESEARCH AND APPLICATIONS

- TRANSATMOSPHERIC VEHICLE FLOW SIMULATION
- SURFACE DIFFUSION
- FLUID DIAGNOSTICS
- CHEMISORPTION
- CATALYSIS
- COMBUSTION
- METALS AND POLYMERS
- AOTV/AFE
- NATIONAL AEROSPACE PLANE/ERV
- LUNAR AND MARS RETURN
- STS/SHUTTLE II
- SPACE STATION

Fig. 1. Objectives of NASA Ames Computational Chemistry Branch.

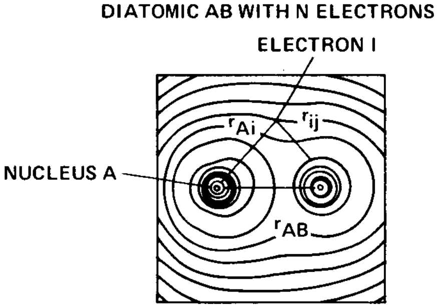
DIATOMIC AB WITH N ELECTRONS
ELECTRON I
NUCLEUS A
r_{Ai}
r_{ij}
r_{AB}

$$\phi_i = \varphi_i \begin{bmatrix} \alpha \\ \beta \end{bmatrix} \qquad \varphi_i = \sum_p c_{ip} X_p$$

$$X_p = \begin{cases} r^{n-1} e^{-\zeta r} Y_{lm} & \text{STO} \\ x^n y^l z^m e^{-\zeta r^2} & \text{GTO} \end{cases}$$

SCHRÖDINGER EQUATION

$$H\Psi_e = \left(-\sum_i^N \left(\frac{1}{2} \nabla_i^2 + \frac{Z_a}{r_{Ai}} + \frac{Z_B}{r_{Bi}} \right) + \sum_{i<j}^N \frac{1}{r_{ij}} \right) \Psi_e = E\Psi_e$$

$$\Psi_e = \sum_{k=1}^{Q} a_k \Phi_k \qquad Q = 10^3 \text{ TO } 10^7$$

$$\Phi_k = \frac{1}{\sqrt{N}} \begin{vmatrix} \phi_1(1)\ \phi_1(2) \dots \phi_1(N) \\ \phi_2(1)\ \phi_2(2) \dots \phi_2(N) \\ \vdots \qquad \vdots \qquad \vdots \\ \phi_N(1)\ \phi_N(2) \dots \phi_N(N) \end{vmatrix}$$

STEPS	ORDER	TIME, sec
SELECT STO OR GTO BASIS	$(M = O(100)$	
COMPUTE INTEGRALS	M^4	400
SORT FOR TRANSFORMATION AND SUPERMATRIX	M^4	100
OBTAIN MOLECULAR ORBITALS SCF OR MCSCF	M^4 OR M^5	60 OR 300
TRANSFORM INTEGRALS TO MO BASIS	M^5	40
CI TO TREAT ELECTRON CORRELATION	M^6	2500
COMPUTE PROPERTIES	M^3	10

Fig. 2. Approach for calculating electronic wave functions for diatomic molecules and typical times on a Cray XMP to execute the calculations.

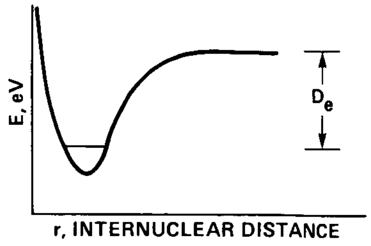

	D_e, eV	
MRSDI + Q	3.457	CH
FCI	3.463	
MRSDI + Q	3.356	NH
FCI	3.355	
MRSDI + Q	4.380	OH
FCI	4.395	

	CH	NH	OH
THIS WORK (COMPUTED)†	3.433	3.344	4.360
THIS WORK (RECOMMENDED)†		3.37 ± 0.03	
EXPERIMENT	3.465	>3.29 <3.47	4.392
MEYER AND ROSMUS CEPA	3.29	3.18	4.11
MEYER AND ROSMUS (ESTIMATE)		3.40	
MELIUS AND BINKLEY		3.35	

† CASSCF/MRSDCI CALCULATIONS BY BAUSCHLICHER AND LANGHOFF

Fig. 3. CASSCF/MRSDCI and full CI calculations on small molecular systems: CH, NH and OH.

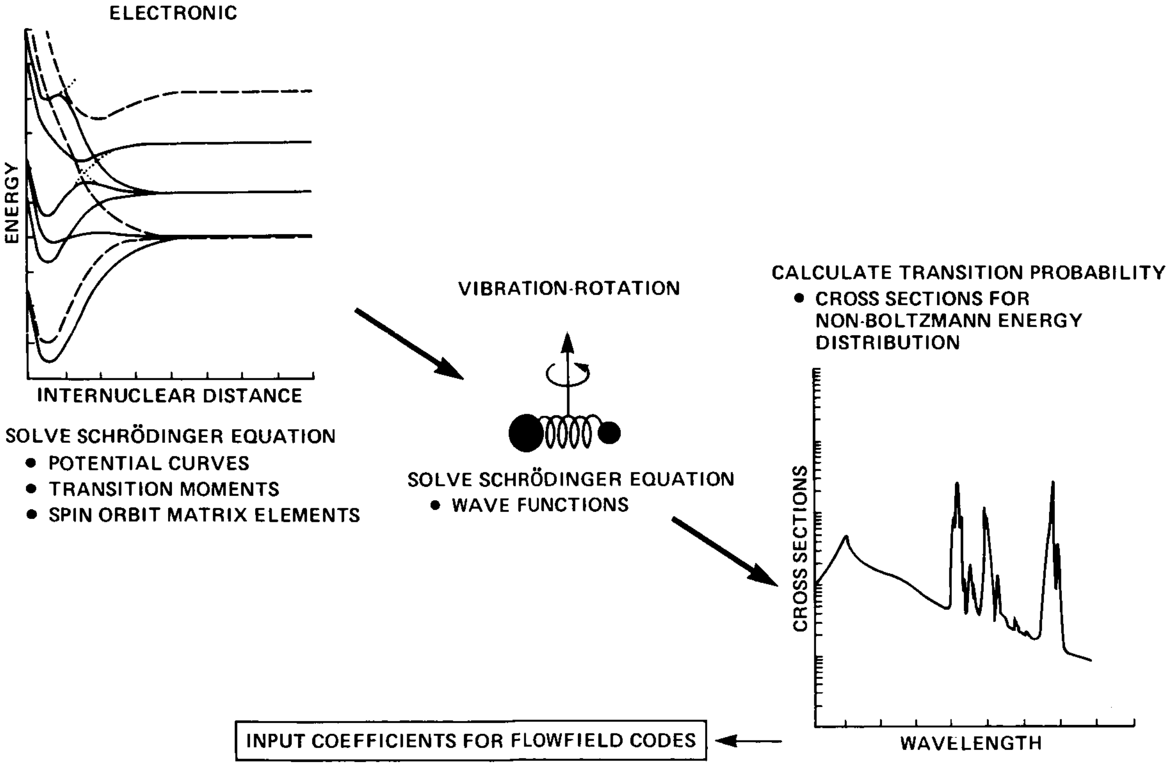
ELECTRONIC
ENERGY
INTERNUCLEAR DISTANCE
SOLVE SCHRÖDINGER EQUATION
• POTENTIAL CURVES
• TRANSITION MOMENTS
• SPIN ORBIT MATRIX ELEMENTS
VIBRATION-ROTATION
SOLVE SCHRÖDINGER EQUATION
• WAVE FUNCTIONS
CALCULATE TRANSITION PROBABILITY
• CROSS SECTIONS FOR NON-BOLTZMANN ENERGY DISTRIBUTION
CROSS SECTIONS
WAVELENGTH
INPUT COEFFICIENTS FOR FLOWFIELD CODES

Fig. 4. Calculation of molecular spectra or optical cross sections from first principles.

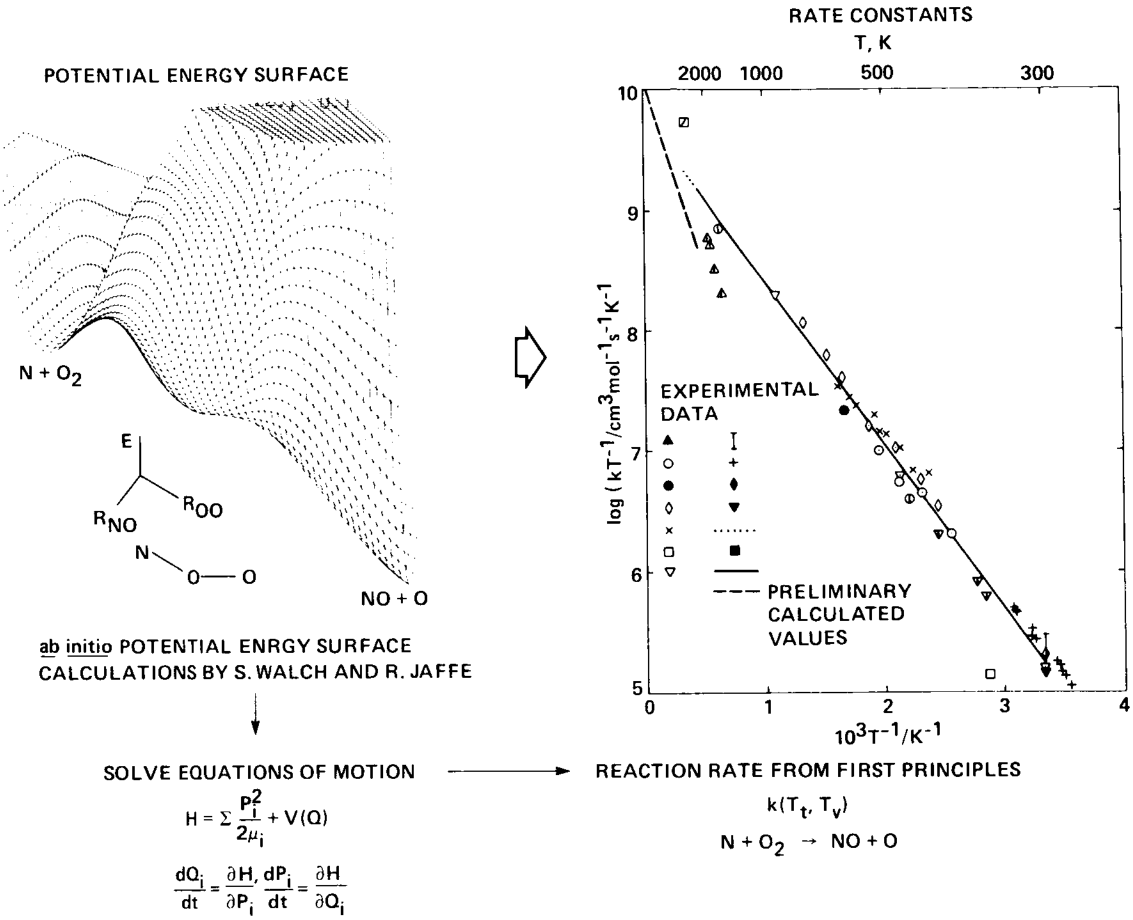
POTENTIAL ENERGY SURFACE
N + O2
NO + O
E
RNO
ROO
N
O — O
ab initio POTENTIAL ENRGY SURFACE CALCULATIONS BY S. WALCH AND R. JAFFE
SOLVE EQUATIONS OF MOTION
H = Σ P_i^2 / 2μ_i + V(Q)
dQ_i/dt = ∂H/∂P_i, dP_i/dt = −∂H/∂Q_i
RATE CONSTANTS
T, K
2000
1000
500
300
10
9
8
7
6
5
0
1
2
3
4
log (kT^-1/cm^3 mol^-1 s^-1 K^-1
10^3 T^-1/K^-1
EXPERIMENTAL DATA
PRELIMINARY CALCULATED VALUES
REACTION RATE FROM FIRST PRINCIPLES
k(T_t, T_v)
N + O2 → NO + O

Fig. 5. Calculations of rate constants for $N+O_2 \rightarrow NO + O$.

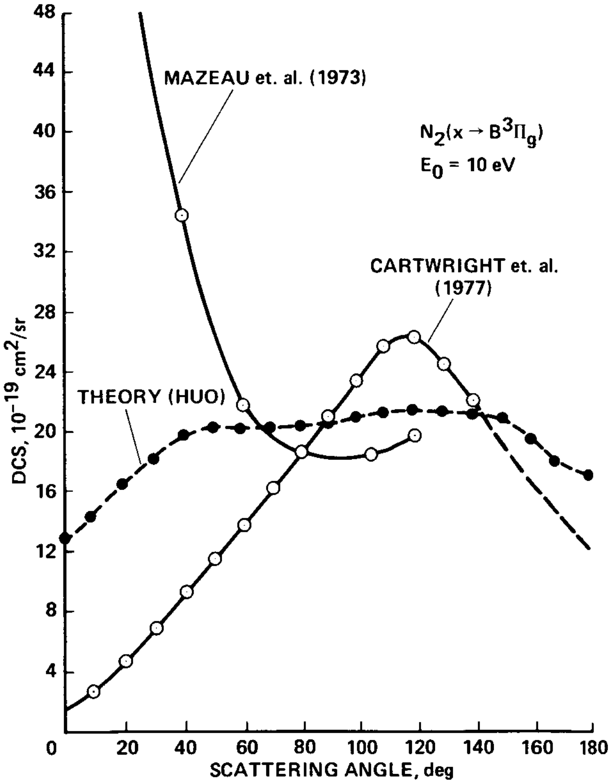

Fig. 6. Differential cross section for $N_2\ X^1\Sigma_g^+ \rightarrow B^3\Pi_g$ by electron impact at 10 eV.

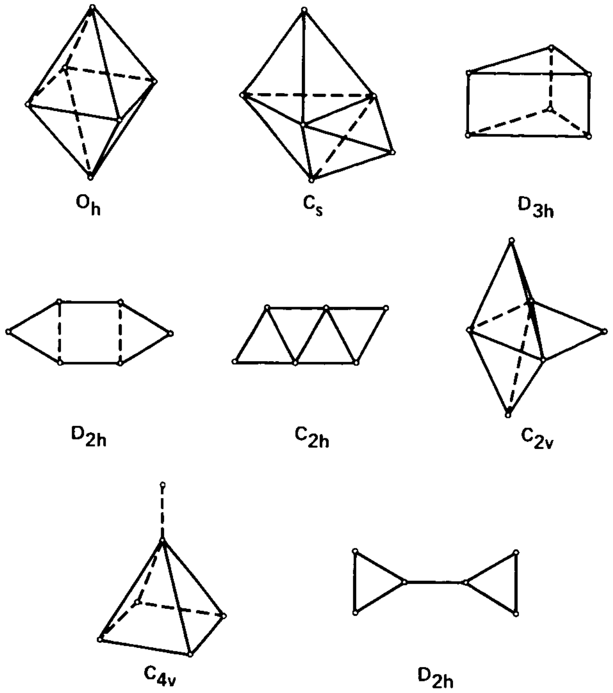
O_h
C_s
D_{3h}
D_{2h}
C_{2h}
C_{2v}
C_{4v}
D_{2h}

Fig. 8. Possible structures constituted of 6 aluminum atoms.

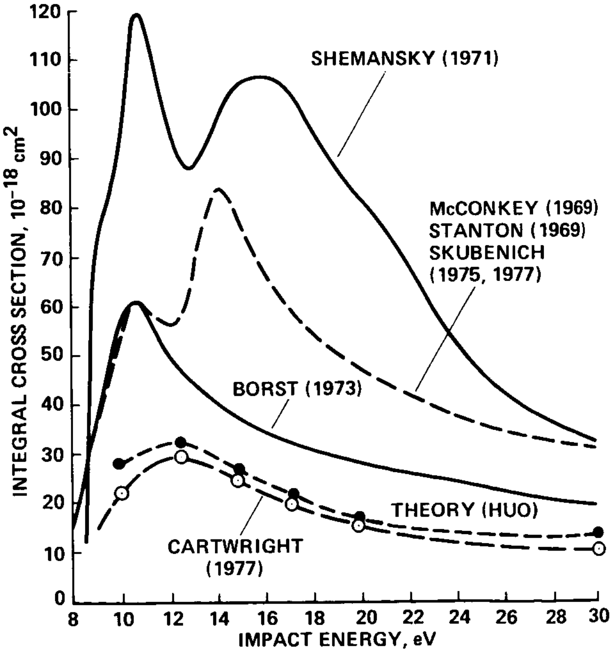

Fig. 7. Total cross section of $N_2\ X^1\Sigma_g^+ \rightarrow B^2\Pi_g$ by electron impact.

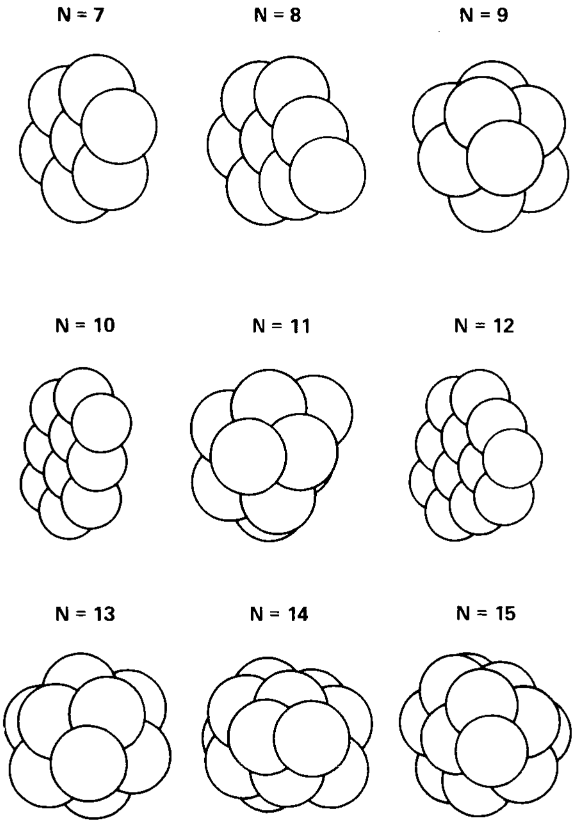
N = 7
N = 8
N = 9
N = 10
N = 11
N = 12
N = 13
N = 14
N = 15

Fig. 9. Lowest-lying structures of aluminum clusters constituted of up to 17 atoms.

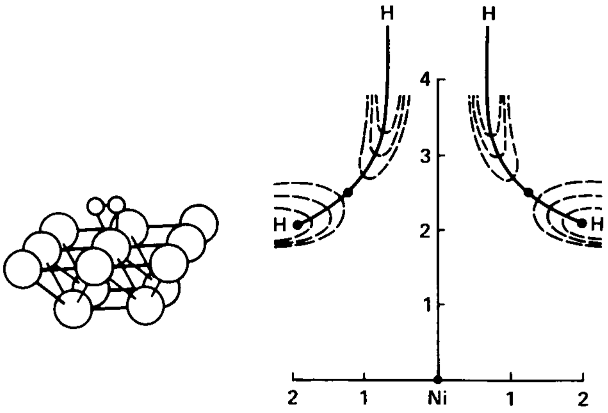

Fig. 10. Computational chemistry study of H_2 dissociation on nickle surface.

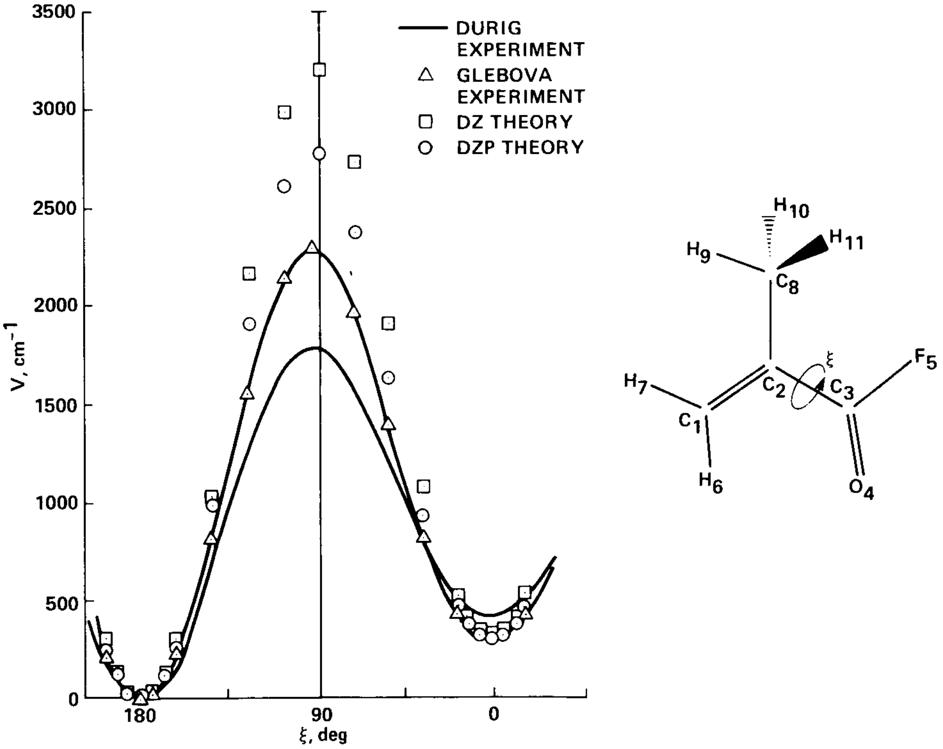

Fig. 11. Energy differences and torsional potential function for Methacryloyl Flouride.

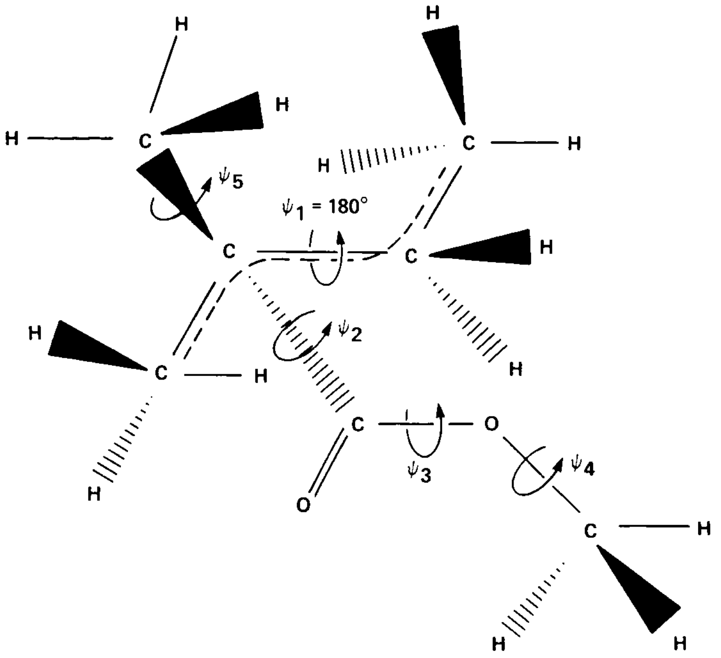
H
H
C
H
ψ5
H
C
H
ψ1 = 180°
C
C
H
H
C
H
ψ2
H
H
C
O
ψ3
O
ψ4
C
H
H
H

Fig. 12. Optimal conformation of 2-Methyl 2-Carbomethoxy butane, a model for a monomeric segment of PMMA.